

Self-Adaptive Probabilistic Skyline Query Processing in Distributed Edge Computing via Deep Reinforcement Learning

Chuan-Chi Lai, *Member, IEEE*

Abstract—In the era of the Internet of Everything (IoE), the exponential growth of sensor-generated data at the network edge renders efficient Probabilistic Skyline Query (PSKY) processing a critical challenge. Traditional distributed PSKY methodologies predominantly rely on pre-defined static thresholds to filter local candidates. However, these rigid approaches are fundamentally ill-suited for the highly volatile and heterogeneous nature of edge computing environments, often leading to either severe communication bottlenecks or excessive local computational latency. To resolve this resource conflict, this paper presents SA-PSKY, a novel Self-Adaptive framework designed for distributed edge-cloud collaborative systems. We formalize the dynamic threshold adjustment problem as a continuous Markov Decision Process (MDP) and leverage a Deep Deterministic Policy Gradient (DDPG) agent to autonomously optimize filtering intensities in real-time. By intelligently analyzing multi-dimensional system states, including data arrival rates, uncertainty distributions, and instantaneous resource availability, our framework effectively minimizes a joint objective function of computation and communication costs. Comprehensive experimental evaluations demonstrate that SA-PSKY consistently outperforms state-of-the-art static and heuristic baselines. Specifically, it achieves a reduction of up to 60% in communication overhead and 40% in total response time, while ensuring robust scalability across diverse data distributions.

Index Terms—Deep Reinforcement Learning, Edge Computing, Multi-Objective Optimization, Probabilistic Skyline Query, Self-Adaptive System, Uncertain Data Streams

I. INTRODUCTION

IN the contemporary landscape of the Internet of Everything (IoE), the explosion of sensor-generated data has shifted the paradigm of data processing from centralized cloud infrastructures to distributed edge nodes [1], [2], [3], [4]. Among various data analysis techniques, the Probabilistic Skyline Query (PSKY) stands out as a critical tool for multi-criteria decision-making under uncertainty [5]. In typical IoE scenarios, such as intelligent transportation systems or industrial monitoring, sensor data are inherently noisy and imprecise [6]. PSKY

This research was supported by the National Science and Technology Council, Taiwan, under Grant No. NSTC 114-2221-E-194-062-. This work was also partially supported by the Advanced Institute of Manufacturing with High-tech Innovations (AIM-HI) from the Featured Areas Research Center Program within the framework of the Higher Education Sprout Project by the Ministry of Education (MOE) in Taiwan. (*Corresponding author: Chuan-Chi Lai*)

C.-C. Lai is with the Department of Communications Engineering, National Chung Cheng University, Minxiong Township, Chiayi County 621301, Taiwan, and also with the Advanced Institute of Manufacturing with High-tech Innovations (AIM-HI), National Chung Cheng University, Minxiong Township, Chiayi County 621301, Taiwan (e-mail: chuanclai@ccu.edu.tw).

addresses this challenge by identifying objects that possess a high likelihood of being optimal based on multiple conflicting attributes, even when their exact values remain unknown or stochastic. However, deploying the PSKY operator within edge environments introduces a fundamental tension between local computational expenditure (especially for high-dimensional skylines [7]) and global communication efficiency [8], [9].

The technical complexity of distributed PSKY processing is primarily centered on the management of the filtering threshold α . This parameter serves as a critical gatekeeper that dictates which local candidate objects possess a sufficiently high probability of belonging to the global skyline set to justify the overhead of transmission to a central broker. In a perfectly stable environment, a static thresholding strategy might provide a reasonable baseline for performance. However, the edge computing ecosystem is characterized by extreme volatility and unpredictable resource availability. Data arrival rates from IoT devices often exhibit bursty patterns, and the statistical distribution of uncertainty, which is represented by the variance and spatial density of data instances, can shift rapidly over short temporal windows [10], [11].

A rigid and pre-defined threshold fails to accommodate these fluctuations, which subsequently leads to two critical forms of system failure. First, an overly conservative threshold results in an information explosion at the network layer. In this situation, redundant data candidates saturate the limited bandwidth and cause excessive queuing delays at the central broker. Second, an overly aggressive threshold significantly reduces the transmission volume but simultaneously imposes a prohibitive computational burden on the CPU of the edge node. This occurs because the system must perform exhaustive instance-level dominance comparisons to satisfy the strict filtering criteria before any data can be discarded. This non-linear relationship between filtering intensity, CPU cycles, and network latency creates a multi-dimensional optimization space that is far too complex for traditional heuristic or rule-based methods to navigate effectively [12], [13], [14].

To overcome these multifaceted challenges, our study introduces a novel Self-Adaptive PSKY (SA-PSKY) framework. Unlike existing methods that rely on manual parameter tuning or simplistic linear control logic [15], [16], the proposed approach leverages Deep Reinforcement Learning (DRL) to achieve autonomous and fine-grained threshold optimization [17]. By transforming the operational state of the edge system into a learnable policy, the SA-PSKY framework can effectively anticipate the impact of threshold adjustments on

the overall system utility. The primary technical contributions of our research, which distinguish it from prior works in both the PSKY and edge computing domains, are summarized into the following three aspects:

- Mathematical Formalization of the Adaptive Pruning Problem: This work provides a rigorous mathematical formulation of the distributed PSKY threshold problem by modeling it as a Markov Decision Process (MDP). This abstraction captures the intricate and non-obvious interdependencies between stochastic data arrival processes, dynamic uncertainty levels, and the hardware resource constraints of the edge nodes.
- Design of a Continuous Action-Space DRL Agent: We develop an intelligent pruning agent based on the Deep Deterministic Policy Gradient (DDPG) algorithm. Unlike discrete reinforcement learning models that often suffer from the curse of dimensionality or quantization errors, this DDPG-based approach enables smooth and continuous adjustment of the threshold α . Such a mechanism ensures that the system can find the exact equilibrium point between computation and communication without the performance oscillations common in discretized control models.
- Comprehensive Performance Analysis and Insights: Beyond presenting raw performance metrics, this paper provides a detailed analysis of how the learned policy adapts to heterogeneous data distributions, such as anti-correlated and independent distributions. This discussion offers practical insights into the underlying trade-offs of intelligent query processing and serves as a blueprint for the deployment of autonomous operators in large-scale, resource-constrained IoT ecosystems.

II. RELATED WORK

The evolution of distributed query processing within IoE environments is characterized by a shift from static centralized models to autonomous edge-cloud collaborative frameworks. This section provides a systematic review of the literature, focusing on the theoretical foundations of skyline queries, distributed architectures, and the application of machine learning in system optimization.

A. Foundations of Skyline Queries over Uncertain Data

The skyline operator was originally introduced as a method for identifying a set of non-dominated objects based on multiple criteria. In the domain of uncertain data, the Probabilistic Skyline Query (PSKY) was developed to handle stochastic attribute values by assigning an existence probability to each object within the skyline set [5]. Early research in this field focused on improving the efficiency of dominance checks through various indexing structures, such as Z-order curves and R-tree variations [18], [19]. To address the challenges posed by continuous data streams, subsequent studies introduced the concept of the sliding window PSKY, which allows for real-time updates of the skyline set as new objects arrive [20], [21]. Further refinements led to the development of the k -dominant skyline and the reverse skyline query, both of which

offer more flexible filtering criteria for complex decision-making scenarios [22], [23], [20]. Despite these advancements, the high computational complexity of calculating exact skyline probabilities remains a significant barrier for real-time applications in resource-constrained environments [24].

B. Distributed and Parallel Processing Architectures

To handle the massive data volumes generated by distributed sensors, research has increasingly focused on parallelizing the skyline operator [25]. Distributed skyline processing typically involves two stages: local pruning at the data sources and global aggregation at a central coordinator [15]. Various partitioning strategies, including grid-based and angle-based partitioning, have been proposed to balance the workload across multiple nodes [26], [27]. In large-scale network environments, peer-to-peer (P2P) architectures were explored to eliminate the single point of failure inherent in centralized brokers [28], [29]. For wireless sensor networks, specific space-efficient algorithms were developed to minimize the memory footprint on nodes while maintaining high query accuracy [30]. Several frameworks [31], [32], [33] have utilized the MapReduce paradigm and Spark-based implementations to achieve scalability in big data environments, though these methods often introduce significant communication latencies that are unsuitable for latency-sensitive IoE tasks. [34] have explored various query types in edge environments, ranging from simple aggregations to complex streaming analytics in satellite networks.

C. Adaptive Resource Management and Edge Computing

The emergence of edge computing has necessitated a more dynamic approach to resource management [35], [14]. Early adaptive systems relied on control theory or heuristic rules to adjust system parameters such as sampling rates and transmission frequencies [36]. Lyapunov optimization techniques were later introduced to provide theoretical guarantees for system stability and energy efficiency under stochastic workloads [37]. In the context of data filtering, some studies proposed rule-based adaptive thresholds that respond to changes in network congestion or CPU utilization [38]. However, these traditional adaptive methods often struggle with the non-linear and high-dimensional nature of modern IoT data streams. Comprehensive surveys on edge-assisted data management highlight that static or simplistic adaptive strategies cannot effectively navigate the complex trade-offs between local computation and global communication in heterogeneous environments [39], [40].

D. Deep Reinforcement Learning for Query Optimization

Deep Reinforcement Learning (DRL) has recently been recognized as a powerful tool for optimizing data management systems. By leveraging the representational power of deep neural networks, DRL agents can learn optimal policies directly from raw system states. In the field of query optimization, DRL has been applied to tasks such as join order selection and index tuning [41]. The transition from discrete models,

like Deep Q-Networks (DQN), to continuous control algorithms, such as Deep Deterministic Policy Gradient (DDPG), has enabled more precise adjustments of system parameters. Recent research has demonstrated the potential of DRL in managing task offloading and bandwidth allocation in edge computing [42]. Furthermore, latest advancements in query processing, such as the efficient algorithms developed for uncertain restricted skyline queries [43], highlight the ongoing necessity for sophisticated optimization techniques to handle complex constraints in probabilistic environments. This work builds upon these advancements by integrating a DDPG based agent into the PSKY framework to achieve fine grained and autonomous control over the filtering threshold in dynamic IoE scenarios.

III. SYSTEM MODEL AND PROBLEM DEFINITION

In this section, we establish the theoretical foundations for probabilistic skyline processing and formalize the joint optimization problem. We model the complex interplay between local edge computation and global cloud communication using queuing theory and computational complexity analysis. To ensure mathematical tractability, the notations used throughout this paper are summarized in Table I. We first introduce the necessary definitions and system assumptions below.

A. Uncertain Data Stream and Statistical Assumptions

Consider a distributed Internet of Everything (IoE) environment where a set of spatially distributed edge nodes, denoted as $\mathcal{E} = \{e_1, e_2, \dots, e_K\}$, continuously collect sensor readings from the physical world. Due to inherent sensing noise, transmission errors, and privacy-preserving perturbations, the collected data is inherently uncertain.

We model each uncertain object $u^{(i)}$ generated at edge node e_i as a set of discrete instances $u^{(i)} = \{u_1^{(i)}, u_2^{(i)}, \dots, u_m^{(i)}\}$. Here, each instance $u_j^{(i)} \in \mathbb{R}^d$ represents a possible state of the object in a d -dimensional feature space, associated with an existence probability $P(u_j^{(i)})$. To ensure statistical consistency within the probability space, we enforce the following normalization constraint:

$$\sum_{j=1}^m P(u_j^{(i)}) \leq 1, \quad (1)$$

where the inequality allows for the possibility that the object may not exist at all (ghost objects).

Assumption 1 (Statistical Independence). We assume that the uncertain objects generated by different sensors are statistically independent. This assumption implies that the probability distributions of any two distinct objects $u^{(i)}$ and $u^{(k)}$ are uncorrelated, allowing their joint probability to be calculated as the product of their individual marginal probabilities.

Definition 1 (Uncertain Data Stream). In the dynamic IoE environment, the raw sensing data generated by an edge node e_i forms an unbounded *Uncertain Data Stream*, denoted as \mathcal{R}_i .

$$\mathcal{R}_i = \langle u^{(1)}, u^{(2)}, \dots, u^{(t)}, \dots \rangle, \quad (2)$$

TABLE I
SUMMARY OF KEY NOTATIONS

Symbol	Description
\mathcal{E}, K	Set of edge nodes $\{e_1, \dots, e_K\}$ and total count
e_i	The i -th edge node ($i \in \{1, \dots, K\}$)
\mathcal{R}_i	Uncertain data stream generated at e_i
u, m, d	Uncertain object, number of instances, dimensions
\mathcal{W}_i	Sliding window set at node e_i
W_{\max}	Maximum capacity of the sliding window
N	Current number of objects in the window ($ \mathcal{W}_i $)
\mathcal{D}_i	Active local dataset ($\mathcal{D}_i = \mathcal{W}_i$)
S_i	Filtered candidate set transmitted from e_i
$P_{\text{sky}}(u)$	Global skyline probability of object u
$P_{\text{local}}(u)$	Local skyline probability computed at edge
$\alpha_{i,t}$	Filtering threshold of node e_i at time t
α_t	Joint action vector $\{\alpha_{1,t}, \dots, \alpha_{K,t}\}$
$\Phi(\alpha)$	Pruning efficiency factor
T_{comp}	Local computation time (Component Latency)
T_{trans}	Data transmission time (Component Latency)
T_{cloud}	Cloud processing and queuing time
L_{sys}	Total end-to-end system latency
ω	Average size of a candidate object (bits)
B	Bandwidth of the shared uplink channel
λ_i, Λ	Local and aggregate data arrival rates
μ	Service rate at the cloud broker
ρ	Traffic intensity (Λ/μ)
s_t, a_t, r_t	State, action, and reward at time step t
w_1, w_2	Weighting coefficients for cost and latency
γ	Discount factor for future rewards
E_{\max}	Maximum training episodes
T_{\max}	Maximum duration of an operational episode

where each $u^{(t)}$ represents an uncertain object arriving at a discrete time step t . The stream is strictly ordered by arrival time, and the volume of data is assumed to be infinite over the system's operational lifespan.

Definition 2 (Sliding Window Model). To process the unbounded stream \mathcal{R}_i under finite memory and latency constraints, each edge node employs a count-based *Sliding Window* mechanism, denoted as \mathcal{W}_i . Let W_{\max} be the maximum capacity of the window. At any given time t , the window $\mathcal{W}_i(t)$ maintains the most recent set of N objects from the stream, where $N \leq W_{\max}$. The window updates follow a First-In-First-Out (FIFO) policy. Let u_{old} denote the oldest object in the window (i.e., the object arriving at time $t - N$). The update rule is:

$$\mathcal{W}_i(t) = \begin{cases} \mathcal{W}_i(t-1) \cup \{u^{(t)}\}, & |\mathcal{W}_i| < W_{\max} \\ (\mathcal{W}_i(t-1) \setminus \{u_{\text{old}}\}) \cup \{u^{(t)}\}, & |\mathcal{W}_i| = W_{\max} \end{cases} \quad (3)$$

Consequently, the local probabilistic skyline computation at time t is performed strictly on the active dataset $\mathcal{D}_i(t) = \mathcal{W}_i(t)$.

B. Probabilistic Dominance and Skyline Definitions

The core concept of skyline queries relies on the dominance relationship. In a deterministic setting, dominance is binary. However, in our uncertain setting, we must quantify the probability that one object is preferable to another.

Definition 3 (Instance-Level Dominance). Let u_A and u_B be two uncertain objects. Let $u_{A,p}$ and $u_{B,q}$ be specific instances

of u_A and u_B respectively in the d -dimensional space. We say $u_{A,p}$ dominates $u_{B,q}$, denoted as $u_{A,p} \prec u_{B,q}$, if and only if $u_{A,p}$ is strictly better (smaller) in at least one dimension and not worse in all other dimensions:

$$\begin{cases} \forall r \in [1, d], \quad v_{A,p,r} \leq v_{B,q,r} \\ \exists r \in [1, d], \quad v_{A,p,r} < v_{B,q,r} \end{cases} \quad (4)$$

where $v_{A,p,r}$ denotes the value of the r -th attribute of instance $u_{A,p}$.

Based on the instance-level comparison, we derive the object-level dominance probability. This metric aggregates the dominance relationships across all possible combinations of instances between two objects.

Definition 4 (Object-Level Dominance Probability). The probability that uncertain object u_A dominates object u_B is defined as the sum of the joint probabilities of all instance pairs where dominance holds:

$$P(u_A \prec u_B) = \sum_{u_{A,p} \in u_A} \sum_{u_{B,q} \in u_B} P(u_{A,p})P(u_{B,q}) \cdot \mathbb{I}(u_{A,p} \prec u_{B,q}), \quad (5)$$

where $\mathbb{I}(\cdot)$ is an indicator function that returns 1 if the dominance condition is met, and 0 otherwise.

Definition 5 (Probabilistic Skyline). An object u is considered a probabilistic skyline candidate if it has a sufficiently high probability of remaining “un-dominated” by the rest of the dataset. Formally, for a global dataset \mathcal{U} , the skyline probability of u is given by:

$$P_{\text{sky}}(u) = \prod_{v \in \mathcal{U}, v \neq u} (1 - P(v \prec u)). \quad (6)$$

If $P_{\text{sky}}(u) \geq \alpha$, where $\alpha \in [0, 1]$ is a user-defined or system-defined filtering threshold, then u is part of the α -Probabilistic Skyline.

C. Distributed Edge-Cloud Architecture

The proposed SA-PSKY framework operates on a two-tier architecture, as illustrated in Fig. 1, designed to minimize the data movement between the edge and the cloud.

1) *Edge Layer (Local Filtering)*: The edge layer consists of heterogeneous edge nodes with limited computational power. Since each node e_i only possesses a local subset of data $\mathcal{D}_i \subset \mathcal{U}$, it cannot calculate the true global skyline probability defined in Eq. (6). Instead, it computes a *Local Skyline Probability* $P_{\text{local}}(u^{(i)})$ based solely on \mathcal{D}_i . Each node maintains the sliding window \mathcal{W}_i , as defined in Section III-A, to process streaming data and applies a local filtering threshold $\alpha_{i,t}$. Objects with $P_{\text{local}}(u^{(i)}) < \alpha_{i,t}$ are pruned immediately, generating a reduced candidate set \mathcal{S}_i . It is important to note that $P_{\text{local}}(u^{(i)}) \geq P_{\text{sky}}(u^{(i)})$; thus, local pruning is safe and does not discard any object that would be part of the final global result (monotonicity property), provided the threshold is managed correctly.

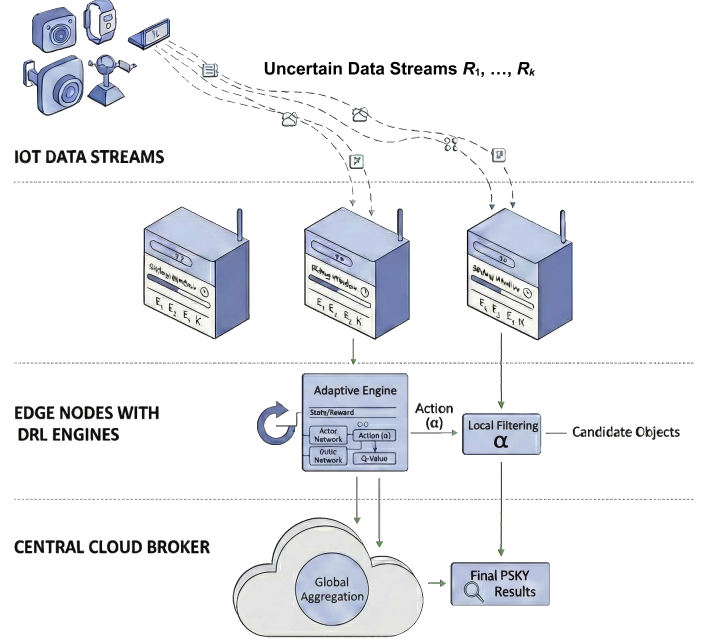


Fig. 1. Distributed Edge-Cloud Architecture for Probabilistic Skyline Query Processing. Each edge node independently filters local data streams before transmitting candidates to a central broker for final aggregation.

2) *Cloud Layer (Global Aggregation)*: The cloud layer hosts a central broker responsible for global verification. It receives the candidate sets $\cup_{i=1}^K \mathcal{S}_i$ from all edge nodes. The broker then performs pairwise dominance checks among candidates from different nodes to compute the final global skyline result.

D. Computational Complexity Model

The computational complexity of probabilistic skyline queries is significantly higher than that of deterministic queries due to the instance-level comparisons. For a local dataset of size N (where $N = |\mathcal{W}_i|$ represents the current sliding window occupancy) with m instances per object, the brute-force complexity is $O(N^2 \cdot m^2 \cdot d)$.

To quantify the impact of the filtering threshold α , we introduce a pruning efficiency factor $\Phi(\alpha) \in (0, 1]$. A higher α allows the algorithm to terminate comparisons earlier (Early Termination), as an object is discarded as soon as its cumulative probability of being dominated exceeds $1 - \alpha$. We model the local computation time T_{comp} for node e_i as:

$$T_{\text{comp}}(e_i, \alpha) = \kappa \cdot N^2 \cdot \Phi(\alpha) \cdot m^2 \cdot d, \quad (7)$$

where κ is a hardware-specific constant reflecting the CPU time per operation. This non-linear relationship implies that increasing α effectively reduces the computational load, but potentially at the cost of higher transmission overhead if too many candidates pass the filter.

E. Network Channel and Queuing Model

In realistic IoE scenarios, edge nodes often share a bandwidth-constrained uplink channel (e.g., LPWAN or shared

5G slice) to communicate with the cloud. We model this contention and the subsequent processing at the broker using queuing theory.

Assumption 2 (Poisson Arrivals): We assume that the arrival of skyline candidates from the distributed edge nodes follows a Poisson process, and the service time at the broker follows an exponential distribution. This allows us to model the system as an M/M/1 queue.

Let ω be the average size of a candidate object (in bits) and B be the total shared bandwidth. The transmission time for node e_i is $T_{\text{trans}}(e_i) = (|S_i(\alpha)| \cdot \omega) / B$. The aggregate arrival rate $\Lambda(\alpha)$ at the cloud is derived as:

$$\Lambda(\alpha) = \sum_{i=1}^K \lambda_i \cdot \sigma_i(\alpha), \quad (8)$$

where λ_i is the raw data generation rate at node e_i , and $\sigma_i(\alpha)$ is the selectivity ratio (the fraction of objects satisfying $P_{\text{local}} \geq \alpha$).

The *Cloud Processing Time* (T_{cloud}), which includes both waiting time in the buffer and service time at the broker, is given by:

$$T_{\text{cloud}}(\alpha) = \frac{1}{\mu - \Lambda(\alpha)}, \quad (9)$$

where μ is the service rate of the broker. To ensure system stability, the traffic intensity must satisfy $\rho = \Lambda(\alpha)/\mu < 1$.

F. Optimization Problem Formulation

The ultimate goal of the SA-PSKY framework is to determine an optimal policy that minimizes the total system expenditure over a specific operational episode. We formalize this as a **finite-horizon** Markov Decision Process (MDP) optimization problem.

1) *System Objective Function:* We define the global objective function J as the expected sum of system-wide costs across a finite sequence of discrete time slots T_{max} :

$$\min_{\pi} J = \mathbb{E} \left[\sum_{t=1}^{T_{\text{max}}} \gamma^{t-1} \cdot C_{\text{total}}(s_t, a_t) \right], \quad (10)$$

where T_{max} represents the maximum duration of an operational episode, and $\gamma \in [0, 1]$ is the discount factor.

2) *Decomposition of Instantaneous Cost:* To balance the trade-off between resource consumption and service delay, the instantaneous cost C_{total} at time step t is decomposed into two weighted components:

$$C_{\text{total}}(t) = w_1 \cdot \underbrace{\sum_{i=1}^K T_{\text{comp}}(i, t)}_{\text{Total Computation Cost}} + w_2 \cdot \underbrace{L_{\text{sys}}(t)}_{\text{System Latency}}, \quad (11)$$

where w_1 and w_2 are weighting coefficients. Note that we use T_{comp} here to represent the computational resource cost (proportional to energy consumption).

Crucially, since the edge nodes operate in parallel but share a constrained communication channel, the *System Latency* $L_{\text{sys}}(t)$ is formulated as:

$$L_{\text{sys}}(t) = \underbrace{\max_i \{T_{\text{comp}}(\alpha_{i,t})\}}_{\text{Parallel Computation}} + \underbrace{\sum_i T_{\text{trans}}(\alpha_{i,t})}_{\text{Shared Transmission}} + T_{\text{cloud}}(\rho_t). \quad (12)$$

Here, the max operator reflects the parallel nature of edge computing, where the system must wait for the slowest node. Conversely, the summation $\sum T_{\text{trans}}$ reflects the bottleneck of the shared uplink bandwidth, where simultaneous data streams are effectively serialized. Finally, T_{cloud} accounts for the queuing and verification time at the broker.

3) *Constraint Set:* The optimization is subject to the following feasibility and stability constraints for each time step $t = 1 \dots T_{\text{max}}$:

$$\text{s.t.} \quad \begin{cases} \alpha_{i,t} \in [\alpha_{\min}, \alpha_{\max}], \quad \forall i \\ \rho_t = \frac{\sum_{i=1}^K \lambda_i \cdot (1 - P_{\text{prune}}(\alpha_{i,t}))}{\mu} < 1. \end{cases} \quad (13)$$

The first constraint limits the action space to a valid probability range. The second constraint guarantees queue stability at the broker.

IV. THE PROPOSED SELF-ADAPTIVE PROBABILISTIC SKYLINE PROCESSING FRAMEWORK

The SA-PSKY framework introduces an autonomous mechanism to navigate the high-dimensional optimization space of distributed filtering. By modeling the coordination between heterogeneous edge nodes and the cloud broker as a Markov Decision Process (MDP), the system achieves a robust balance between local computational load and global communication latency.

A. MDP Formulation for Threshold Control

We formalize the interaction between the edge-assisted query operator and the dynamic sensing environment as a tuple $(\mathcal{S}, \mathcal{A}, \mathcal{R}, \gamma)$.

- **State Space (\mathcal{S}):** The state vector s_t at time t provides a multi-faceted representation of the system status:

$$s_t = \{\boldsymbol{\lambda}_t, \boldsymbol{\sigma}_t, \mathcal{D}_t, B_t, Q_t\}, \quad (14)$$

where $\boldsymbol{\lambda}_t$ denotes the vector of data arrival rates, $\boldsymbol{\sigma}_t$ represents the uncertainty variances, \mathcal{D}_t is the distribution density (e.g., correlated or anti-correlated), B_t is the instantaneous bandwidth, and Q_t signifies the current broker queue status.

- **Action Space (\mathcal{A}):** The action a_t corresponds to the adjustment of the threshold vector $\boldsymbol{\alpha}_t = \{\alpha_{1,t}, \dots, \alpha_{K,t}\}$. Unlike discrete models, SA-PSKY utilizes a continuous action space where each $\alpha_{i,t} \in [\alpha_{\min}, \alpha_{\max}]$, allowing for infinitesimal adjustments to the pruning intensity.
- **Reward Function (\mathcal{R}):** The reward r_t is the negative reflection of the instantaneous system cost defined in

Section III. To align with the objective function in Eq. (10), it is formulated as:

$$r_t = -C_{\text{total}}(t) + \mathcal{P}(\rho_t), \quad (15)$$

where $C_{\text{total}}(t)$ is the weighted cost composed of computation and system latency (Eq. 11), and $\mathcal{P}(\rho_t)$ is a penalty term that applies a heavy cost if the traffic intensity $\rho_t \geq 1$, ensuring system stability.

B. Deep Deterministic Policy Gradient Architecture

The continuous nature of the threshold adjustment problem necessitates an Actor-Critic architecture. The SA-PSKY agent employs four distinct neural networks: the actor $\mu(s|\theta^\mu)$, the critic $Q(s, a|\theta^Q)$, and their respective target networks μ' and Q' .

- **Actor Network:** This network parameterizes the policy by mapping states to deterministic actions. It consists of an input layer, three hidden layers with ReLU activation, and a Sigmoid output layer to ensure $\alpha \in [0, 1]$.
- **Critic Network:** The critic approximates the action-value function $Q(s, a)$. To capture the non-linear coupling between state variables and actions, the action vector is concatenated with the state features in the second hidden layer.

C. Reward Mechanism for Multi-Objective Balance

A primary challenge in distributed IoE environments is the disparate scales of computational and communication costs. To address this, we implement a normalized reward structure based on Eq. (11) and Eq. (12):

$$r_t = - \left(w_1 \cdot \frac{\sum_i T_{\text{comp}}(i, t)}{C_{\text{max}}} + w_2 \cdot \frac{L_{\text{sys}}(t)}{L_{\text{max}}} \right), \quad (16)$$

where C_{max} and L_{max} are normalization constants derived from initial system profiling. The weights w_1 and w_2 are dynamically configurable. For example, in energy-constrained edge scenarios, w_1 can be increased to prioritize CPU conservation, thereby forcing the agent to adopt a more moderate pruning policy.

D. Policy Optimization and Stability Mechanisms

The SA-PSKY agent utilizes the Actor-Critic architecture to iteratively refine its threshold control policy. The Critic network, parameterized by θ^Q , approximates the optimal Q -function by minimizing the Mean Squared Bellman Error (MSBE) over a mini-batch of M transitions:

$$L(\theta^Q) = \frac{1}{M} \sum_{j=1}^M (y_j - Q(s_j, a_j|\theta^Q))^2, \quad (17)$$

where $y_j = r_j + \gamma Q'(s_{j+1}, \mu'(s_{j+1}|\theta^{\mu'})|\theta^Q)$ is the target value for the j -th sample. Simultaneously, the Actor network, parameterized by θ^μ , is updated to maximize the expected return via the sampled policy gradient:

$$\nabla_{\theta^\mu} J \approx \frac{1}{M} \sum_{j=1}^M \nabla_a Q(s, a|\theta^Q)|_{s=s_j, a=\mu(s_j)} \nabla_{\theta^\mu} \mu(s|\theta^\mu)|_{s_j}. \quad (18)$$

TABLE II
SA-PSKY HYPER-PARAMETER SETTINGS

Parameter	Value
Hidden Layers (Actor/Critic)	3 (400, 300, 200 neurons)
Activation Function	ReLU (Hidden), Sigmoid (Output)
Learning Rate Actor (η_μ)	10^{-4}
Learning Rate Critic (η_Q)	10^{-3}
Discount Factor (γ)	0.99
Soft Update (τ)	0.005
Replay Buffer Size	10^6
Mini-batch Size (M)	128

To ensure stable training and rapid convergence in non-stationary IoE environments, the framework incorporates the following two mechanisms:

- **Prioritized Experience Replay:** Instead of uniform sampling, we implement a prioritized experience replay buffer \mathcal{B} . Each transition is assigned a priority based on its temporal-difference (TD) error, allowing the agent to learn more effectively from rare but critical system states, such as sudden network congestion.
- **Soft Target Updates:** To prevent the policy from oscillating due to rapid shifts in target values, the target networks $\theta^{\mu'}$ and $\theta^{Q'}$ are updated using a soft tracking mechanism:

$$\begin{cases} \theta^{Q'} \leftarrow \tau \theta^Q + (1 - \tau) \theta^{Q'} \\ \theta^{\mu'} \leftarrow \tau \theta^\mu + (1 - \tau) \theta^{\mu'} \end{cases} \quad (19)$$

where $\tau \ll 1$ is the target smoothing coefficient (e.g., $\tau = 0.005$). This incremental update ensures that the target values shift gradually, which is critical for maintaining decision consistency in time-sensitive edge computing environments.

E. Exploration via Ornstein-Uhlenbeck Process

In threshold control, random white noise is often insufficient due to the temporal correlation of data streams. We employ the Ornstein-Uhlenbeck (OU) process \mathcal{N}_t to inject temporally correlated noise into the action selection:

$$a_t = \text{clip}(\mu(s_t|\theta^\mu) + \mathcal{N}_t, \alpha_{\min}, \alpha_{\max}). \quad (20)$$

The OU process provides mean-reverting behavior, which ensures that the agent explores the threshold space smoothly, allowing the system to observe the long-term impact of threshold shifts on the broker's queue length.

F. Neural Architecture and Hyper-parameter Configuration

To ensure robust performance across heterogeneous hardware, we adopt a deep architecture for both networks. The Specific layers and configurations are detailed to provide reproducibility. Both the actor and critic networks utilize three fully connected hidden layers with 400, 300, and 200 neurons respectively. The specific hyper-parameters are summarized in Table II.

G. Algorithmic Implementation and Training Procedure

The implementation follows an off-policy training regime to ensure high sample efficiency. The complete training procedure is outlined in Algorithm 1, which orchestrates the interaction between the edge-based DDPG agent and the IoE environment. The process is structurally divided into three key phases:

1) *Phase 1: Initialization (Lines 1–3):* The procedure commences by initializing the primary Actor network $\mu(s|\theta^\mu)$ and Critic network $Q(s, a|\theta^Q)$ with random weights. To stabilize the learning process and preventing the divergence of value estimation, we create copies of these networks, denoted as target networks $\theta^{\mu'}$ and $\theta^{Q'}$. Additionally, a prioritized replay buffer \mathcal{B} is instantiated to store transition tuples, allowing the agent to learn from historical experiences rather than solely consecutive samples.

2) *Phase 2: Interaction and Exploration (Lines 5–9):* At each time step t , the agent observes the current system state s_t (comprising data arrival rate, queue length, etc.). To encourage exploration in the continuous action space, Ornstein-Uhlenbeck (OU) noise \mathcal{N}_t is added to the deterministic action generated by the Actor (Line 6). The resulting action a_t is clipped to the valid range $[\alpha_{\min}, \alpha_{\max}]$ and executed as the filtering threshold vector α_t . The system then transitions to s_{t+1} and returns a reward r_t . This transition tuple (s_t, a_t, r_t, s_{t+1}) is stored in buffer \mathcal{B} with maximal priority to ensure it is replayed frequently in the early stages.

3) *Phase 3: Network Optimization (Lines 11–18):* Once the buffer \mathcal{B} accumulates sufficient samples, the dual-optimization loop begins.

- **Critic Update (Lines 13–14):** A mini-batch of M transitions is sampled. The Critic minimizes the Mean Squared Bellman Error (MSBE) between the predicted Q-value and the target value y_j . The target y_j is computed using the Bellman equation, incorporating the reward and the discounted future value estimated by the target networks.
- **Actor Update (Line 16):** The Actor is updated via the deterministic policy gradient method. The gradient $\nabla_{\theta^\mu} J$ is calculated by chaining the gradient of the Critic with respect to the action and the gradient of the Actor with respect to its parameters. This step effectively adjusts the policy to produce actions that maximize the Q-value.
- **Soft Update (Lines 17–18):** Finally, the weights of the target networks are slowly tracked towards the primary networks using a soft update coefficient τ (e.g., $\tau = 0.005$). This ensures that the target values change slowly, thereby smoothing the training dynamics.

H. Computational Complexity and Pruning Efficiency

The computational overhead at each edge node is predominantly determined by the complexity of the probabilistic dominance checks. For a local dataset of size N (where $N \leq W_{\max}$ represents the current active objects in the window) with m discrete instances across d dimensions, the brute-force complexity is $O(N^2 \cdot m^2 \cdot d)$. This high complexity necessitates an efficient pruning mechanism.

Algorithm 1: SA-PSKY Threshold Optimization via DDPG

Input : Initial state s_1 , Max episodes E_{\max} , Max steps T_{\max} , Learning rates η_μ, η_Q , Soft update τ , Discount factor γ
Output: Optimized Policy Parameters θ^μ , Critic Parameters θ^Q

```

// Phase 1: Initialization
1 Initialize Actor  $\mu(s|\theta^\mu)$  and Critic  $Q(s, a|\theta^Q)$  with
  random weights;
2 Initialize target networks  $\theta^{\mu'} \leftarrow \theta^\mu$  and  $\theta^{Q'} \leftarrow \theta^Q$ ;
3 Initialize prioritized experience replay buffer  $\mathcal{B}$  and
  exploration noise  $\mathcal{N}$ ;
```

for $episode = 1$ **to** E_{\max} **do**

Reset IoE environment and receive initial state s_1 ;

for $t = 1$ **to** T_{\max} **do**

// Phase 2: Interaction

Select action

$a_t = \text{clip}(\mu(s_t|\theta^\mu) + \mathcal{N}_t, \alpha_{\min}, \alpha_{\max})$;

Execute action a_t (set local thresholds

$\alpha_t = a_t$);

Observe joint reward r_t and transition to s_{t+1} ;

Store transition (s_t, a_t, r_t, s_{t+1}) in \mathcal{B} with
 initial priority;

if $\text{size of } \mathcal{B} > \text{Batch Size } M$ **then**

// Phase 3: Optimization

Sample a mini-batch of M transitions from
 \mathcal{B} indexed by j ;

Set target value

$y_j = r_j + \gamma Q'(s_{j+1}, \mu'(s_{j+1}|\theta^{\mu'})|\theta^{Q'})$;

// Update Critic Network

Update Critic by minimizing MSBE Loss:

$L = \frac{1}{M} \sum_{j=1}^M (y_j - Q(s_j, a_j|\theta^Q))^2$;

// Update Actor Network

$\nabla_{\theta^\mu} J \approx$

$\frac{1}{M} \sum_{j=1}^M \nabla_a Q(s, a|\theta^Q)|_{s=s_j, a=\mu(s_j)} \nabla_{\theta^\mu} \mu(s|\theta^\mu)|_{s_j}$;

// Soft Update Target Networks

$\theta^{\mu'} \leftarrow \tau \theta^\mu + (1 - \tau) \theta^{\mu'}$;

$\theta^{Q'} \leftarrow \tau \theta^Q + (1 - \tau) \theta^{Q'}$;

end

$s_t \leftarrow s_{t+1}$;

end

// Decay exploration noise

Update \mathcal{N} parameters for the next episode;

end

By introducing the filtering threshold α , the SA-PSKY framework effectively reduces the search space. Let N_α be the number of objects whose local skyline probability exceeds the threshold ($N_\alpha \ll N$). The average-case complexity is subsequently reduced to $O(N \cdot N_\alpha \cdot m^2 \cdot d)$. This theoretical reduction illustrates that the filtering threshold is a critical regulator of local CPU utilization. As the data distribution

TABLE III
SIMULATION PARAMETERS

Parameter	Value
Total Data Volume	50,000 objects
Number of Edge Servers	5
Average Object Size	1 Kbit
Network Bandwidth	1 Mbps
Default Instances per Object (m)	3
Default Data Dimensions (d)	3
Sliding Window Capacity (W_{\max})	500
Baseline Fixed Thresholds	$\alpha = 0.02$

shifts, the value of N_α typically increases, which forces the DRL agent to adjust α more aggressively to prevent computational saturation. This relationship reinforces the necessity of the multi-objective reward function, which balances these non-linear computational costs (T_{comp}) against communication latencies (T_{trans}).

V. EXPERIMENTAL EVALUATION

In this section, we conduct a comprehensive evaluation of the proposed SA-PSKY framework. A critical aspect of this study is to analyze the trade-off between the computationally intensive dominance checks required for uncertain data and the constrained network bandwidth inherent in IoE environments.

A. Simulation Environment and Settings

The simulation setup includes $K = 5$ edge servers and one cloud broker processing 50,000 uncertain objects. The network bandwidth is restricted to 1 Mbps to simulate a congested uplink. The average object size is set to 1 Kbit. Crucially, processing uncertain data involves probabilistic dominance checks with a time complexity of $O(N^2 \cdot m^2)$, where m is the number of instances. This makes the computation latency a non-negligible factor in the end-to-end performance.

The key parameters used in the experiments are listed in Table III. An ϵ -greedy strategy (with $\epsilon = 0.8$ initially) is employed to balance exploration and exploitation.

We compare the performance of SA-PSKY against the following baseline strategies:

- 1) **No-Filtering (Centralized):** All uncertain objects are transmitted to the cloud broker. This represents the worst-case scenario for communication cost.
- 2) **Fixed-Threshold:** The edge nodes apply a static filtering probability (tested with $\alpha = 0.02$). This baseline evaluates the performance of non-adaptive pruning.

B. Default Performance Evaluation

To conduct a granular analysis of the system performance, we decompose the End-to-End Latency (T_{total}) into its constituent components: Transmission Latency (T_{trans}) and Computation Latency (T_{comp}).

1) *Transmission Latency Analysis (T_{trans})*: Fig. 2(a) isolates the latency incurred strictly from data transmission across the different methods under default settings.

- **No-Filtering:** Transmitting the full raw dataset of 50,000 objects (approx. 50 Mbits) over the constrained 1 Mbps

uplink results in a prohibitive transmission bottleneck of approximately **42.5 seconds**. This value empirically aligns with the theoretical bandwidth limit, confirming that the channel is fully saturated.

- **Fixed-Threshold:** By applying a static threshold ($\alpha = 0.02$), the system filters out approximately 30% of the objects. While this alleviates some pressure, the remaining data volume still incurs a significant transmission delay of approximately **31 seconds**.
- **SA-PSKY:** The DRL agent dynamically identifies and prunes dominated objects with high precision. By filtering out approximately 60% of the data at the edge, the transmission latency is drastically reduced to approximately **12 seconds**, effectively preventing network congestion.

2) *Computation Latency Analysis (T_{comp})*: Given the $O(N^2)$ complexity of probabilistic skyline queries, computational overhead is a dominant factor in the total latency budget. Fig. 2(b) illustrates the processing time required for dominance checks across different strategies.

- **Centralized Bottleneck (No-Filtering):** In the centralized approach, the cloud broker executes global dominance checks on the entire unprocessed dataset of 50,000 objects. This centralization creates a single point of failure and a prohibitive computational bottleneck, resulting in a latency of approximately **230 seconds**.
- **Fixed-Threshold:** Although edge nodes reduce the dataset size via static filtering, the residual candidate set remains substantial. Consequently, the cloud broker still faces a heavy workload, leading to a serialized computation time of approximately **125 seconds**.
- **Adaptive-Threshold (SA-PSKY):** SA-PSKY shifts the computational paradigm from centralized execution to distributed parallelism. The dominance checks are partitioned across $K = 5$ edge nodes, with each node processing a smaller subset (approx. 10,000 objects). Although the aggregate CPU cycles remain high, the effective wall-clock time is determined by the slowest edge node. This parallel execution significantly reduces the computation latency to approximately **70 seconds**.

3) *End-to-End System Latency Analysis (T_{total})*: Fig. 2(c) aggregates the performance metrics to present the total end-to-end system latency. Consistent with the theoretical model defined in (12), the total latency L_{sys} is the sum of the effective parallel computation time and the serialized transmission delay:

$$L_{\text{sys}} \approx \underbrace{\max_i \{T_{\text{comp}}(e_i)\}}_{\text{Parallel Edge Processing}} + \underbrace{\sum_i T_{\text{trans}}(e_i)}_{\text{Serialized Transmission}} .$$

It is important to note that the theoretical queuing delay $L_{\text{queue}}(\rho_t)$ is implicitly captured within the serialized transmission term. Since the shared channel forces a sequential upload order, the waiting time for network access is mathematically equivalent to the summation of transmission durations. Furthermore, due to the strict bandwidth bottleneck (1 Mbps), the data arrival rate at the broker is significantly lower than

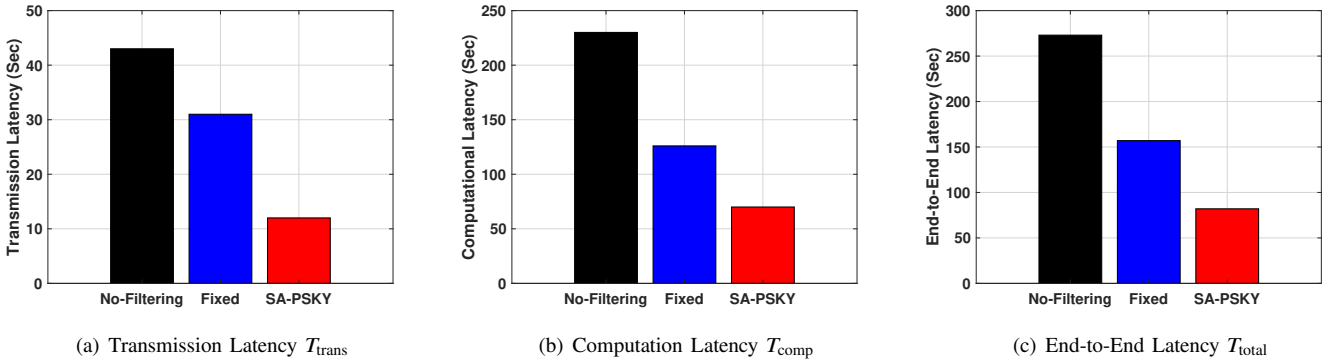


Fig. 2. Comparison of different methods under default settings in terms of: (a) Transmission Latency T_{trans} , (b) Computation Latency T_{comp} , and (c) End-to-End Latency T_{total} .

its service rate, rendering the internal cloud processing queue negligible.

The comparative results reveal a stark contrast in architectural efficiency:

- **No-Filtering:** This approach is penalized by both communication and computation bottlenecks. The serialized transmission of 50 Mbits incurs 42.5 seconds, while the sequential processing of the full dataset at the cloud adds 230 seconds. This results in a worst-case total latency of approximately **273 seconds**.
- **Fixed-Threshold:** While static filtering reduces transmission time to 31 seconds, it fails to sufficiently reduce the computational burden on the cloud, leading to a suboptimal total latency of approximately **156 seconds**.
- **SA-PSKY:** By offloading computation to the edge, our framework introduces a local processing cost. However, this investment yields a critical dual benefit:

- 1) **Data Reduction:** The intelligent pruning reduces the serialized transmission term ($\sum T_{\text{trans}}$) significantly to approximately **12 seconds**.
- 2) **Parallel Computing:** The computationally expensive dominance checks are executed in parallel across the edge nodes. The system latency is thus governed by the parallel execution time ($\max T_{\text{comp}} \approx 70\text{s}$), which is far lower than the serialized cloud execution time.

Consequently, SA-PSKY achieves a total end-to-end latency of approximately **82 seconds**.

In summary, SA-PSKY achieves a total latency reduction of approximately **70%** compared to the centralized baseline. This confirms that offloading expensive computation to parallel edge nodes is not merely a bandwidth-saving strategy, but a necessary architectural choice to mitigate the bottlenecks defined in Section III.

C. Impact of Instances per Uncertain Object (m)

In the preceding subsections, we established that the Centralized (No-Filtering) approach suffers from prohibitive latency due to bandwidth bottlenecks. Consequently, including it in further sensitivity analyses would obscure the nuanced

performance differences between the edge-based strategies. Therefore, in the following experiments, starting with the impact of instance count m , we omit the Centralized baseline to focus strictly on the comparison between the proposed SA-PSKY and the Fixed-Threshold mechanisms.

We first investigate the robustness of the system against data uncertainty by varying the number of instances m per object from 3 to 9. We maintain all other parameters at their default settings as specified in Table III. A higher m value indicates greater uncertainty, which theoretically increases the complexity of dominance checks by a factor of m^2 . The experimental results regarding transmission, computation, and end-to-end latency are presented in Fig. 3.

As the number of instances increases, the difficulty of dominance checking rises significantly. The results reveal three key observations:

- **Transmission Latency (T_{trans}):** As shown in Fig. 3(a), the Fixed-Threshold approach maintains a relatively constant but high transmission latency across all m values. In contrast, SA-PSKY exhibits an interesting adaptive behavior where the transmission latency actually decreases from approximately 17 seconds to 10 seconds as m increases. This indicates that the DRL agent intelligently detects the rising cost of processing complex objects and proactively tightens the filtering threshold to reduce data volume.
- **Computation Latency (T_{comp}):** Fig. 3(b) demonstrates the impact of the quadratic complexity. The computation time for the Fixed-Threshold method grows exponentially, soaring from approximately 150 seconds at $m = 3$ to nearly 950 seconds at $m = 9$. Conversely, SA-PSKY effectively dampens this growth. By distributing the workload and aggressively pruning complex objects, it limits the computation latency to approximately 420 seconds in the worst-case scenario.
- **End-to-End Scalability (T_{total}):** Consequently, Fig. 3(c) shows that the performance gap between the two methods widens as data uncertainty increases. While the Fixed-Threshold approach fails to adapt to the computational surge, causing extreme system delays, SA-PSKY demonstrates superior scalability. The agent autonomously balances the trade-off between local filtering and global

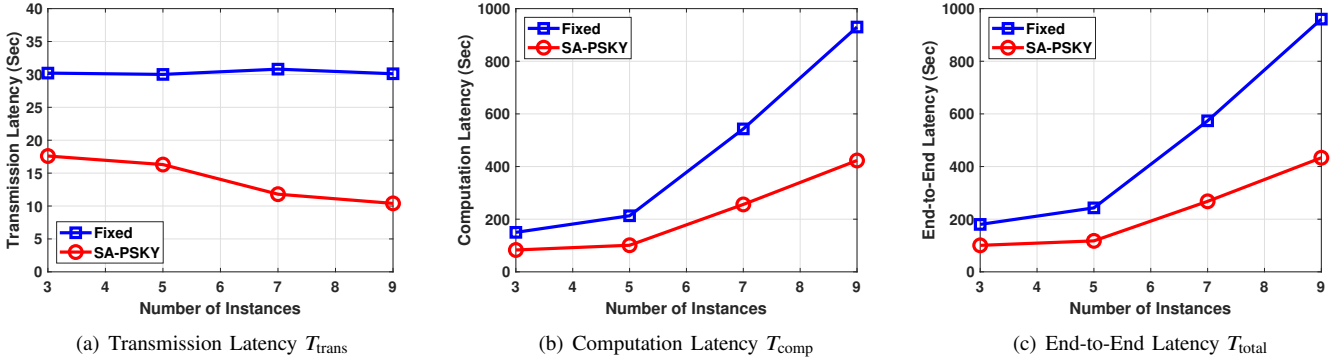


Fig. 3. Comparisons of different methods under varying number of instances per uncertain object (m) in terms of: (a) Transmission Latency T_{trans} , (b) Computation Latency T_{comp} , and (c) End-to-End Latency T_{total} .

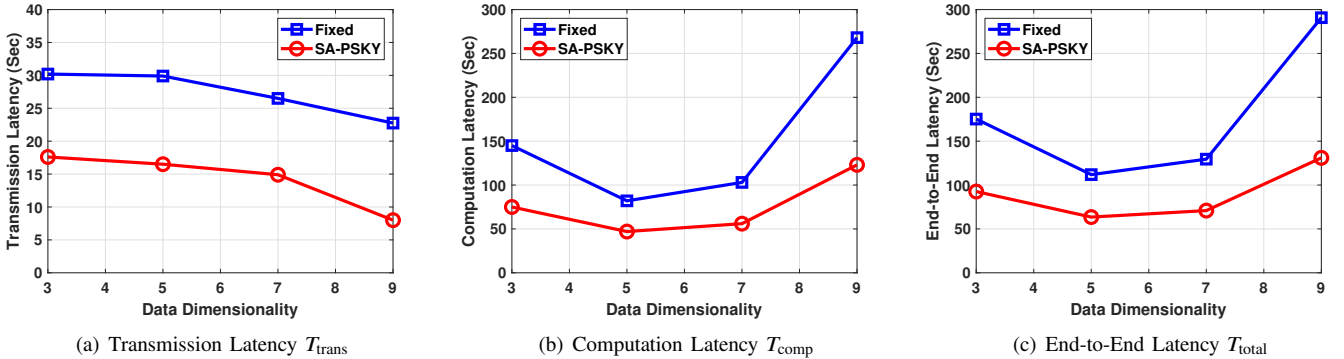


Fig. 4. Comparisons of different methods under varying data dimensionality per uncertain object (d) in terms of: (a) Transmission Latency T_{trans} , (b) Computation Latency T_{comp} , and (c) End-to-End Latency T_{total} .

processing, maintaining a stable system response time even as the intrinsic data complexity rises.

D. Impact of Data Dimensionality (d)

Following the analysis of instance uncertainty, we further examine the impact of data dimensionality d on system performance. We vary the number of attributes d from 3 to 9 while keeping other parameters at their default values. The "Curse of Dimensionality", a well-known challenge in parallel skyline processing [7], typically presents a dual challenge: it increases the computational cost of each pairwise comparison linearly ($O(d)$) and often alters the dominance relationships, potentially inflating the skyline size. The experimental results are summarized in Fig. 4.

The results in Fig. 4 illustrate how the system copes with high-dimensional uncertainty.

- **Transmission Latency (T_{trans}):** As illustrated in Fig. 4(a), the transmission latency for both methods exhibits a downward trend as dimensionality increases. For the Fixed-Threshold approach, the latency decreases from approximately 30 seconds at $d = 3$ to 23 seconds at $d = 9$. This phenomenon occurs because, in high-dimensional probabilistic spaces, it becomes statistically more difficult for an object to maintain a high "skyline probability" across all dimensions simultaneously, causing more ob-

jects to naturally fall below the filtering threshold. SA-PSKY exploits this characteristic even further. The agent learns that high-dimensional objects are computationally expensive to process at the cloud, so it proactively tightens the pruning policy, reducing the transmission latency to approximately 8 seconds at $d = 9$.

- **Computation Latency (T_{comp}):** Fig. 4(b) reveals a non-monotonic trend. Initially, from $d = 3$ to $d = 5$, the computation time decreases for both methods. This correlates with the reduction in transmitted data volume observed in Fig. 4(a), as fewer candidates require dominance checks. However, as dimensionality increases to $d = 7$ and $d = 9$, the "Curse of Dimensionality" becomes the dominant factor. The Fixed-Threshold method suffers a sharp performance degradation, with computation time skyrocketing to nearly 270 seconds at $d = 9$ due to the increased cost of per-object attribute comparisons. In contrast, SA-PSKY effectively mitigates this surge. By aggressively filtering candidates at the edge, it keeps the cloud workload manageable, capping the computation latency at approximately 120 seconds.
- **End-to-End Latency (T_{total}):** Fig. 4(c) confirms the superior scalability of the proposed framework. While the Fixed-Threshold approach becomes unstable at high dimensions due to computational saturation, SA-PSKY maintains a robust performance profile. The DRL agent

successfully navigates the trade-off, accepting a slightly stricter local filtering policy to prevent the cloud broker from being overwhelmed by complex high-dimensional dominance checks.

E. Summary of Experimental Findings

The comprehensive evaluation presented in this section validates the efficacy and robustness of the proposed SA-PSKY framework across varying system conditions. The key takeaways are summarized as follows:

- 1) **Architectural Superiority:** Our results confirm that the traditional Centralized approach is fundamentally ill-suited for bandwidth-constrained IoE environments, suffering from prohibitive latencies (up to 273 seconds). By offloading computation to the edge, SA-PSKY successfully breaks the communication bottleneck. Although this introduces local computational overhead, the parallel processing capability of the distributed edge nodes ensures that the total end-to-end latency is reduced by approximately **70%** under default settings.
- 2) **Intelligent Adaptation:** Unlike the Fixed-Threshold approach, which requires manual tuning and fails to adapt to dynamic workload shifts, the DRL-based agent in SA-PSKY demonstrates autonomous adaptability. It effectively learns the complex non-linear relationship between data characteristics (e.g., uncertainty levels, dimensionality) and system resource constraints. As evidenced in Fig. 3 and Fig. 4, the agent proactively tightens filtering policies during high-load scenarios to prevent system saturation.
- 3) **Robust Scalability:** The framework exhibits superior scalability when facing high data uncertainty (high m) and dimensionality (high d). While baseline methods degrade exponentially due to the $O(N^2)$ and "Curse of Dimensionality" effects, SA-PSKY maintains a stable response time. This stability is achieved by dynamically balancing the trade-off between local pruning intensity and global aggregation overhead, making it a viable solution for real-time analytics in large-scale IoE networks.

These findings collectively demonstrate that SA-PSKY not only solves the immediate latency problem but also provides a resilient foundation for processing uncertain data streams in heterogeneous edge computing environments.

VI. CONCLUSION

This paper presented SA-PSKY, a self-adaptive framework designed to resolve the critical tension between computational resource consumption and communication bandwidth in distributed probabilistic skyline query processing. Unlike traditional static filtering mechanisms that fail to adapt to the volatility of IoE data streams, SA-PSKY formulates the threshold selection problem as a continuous control task within a Markov Decision Process. By leveraging the Deep Deterministic Policy Gradient (DDPG) algorithm, the proposed framework empowers edge nodes to autonomously learn optimal pruning policies. This mechanism effectively orchestrates a

fine-grained trade-off between local processing overhead and global transmission latency.

Experimental results demonstrate that SA-PSKY significantly outperforms existing centralized and fixed-threshold baselines, achieving an end-to-end latency reduction of approximately 70% under default settings. Crucially, the framework exhibits robust scalability in high-dimensional and highly uncertain data environments, successfully mitigating the "curse of dimensionality" that typically paralyzes conventional skyline algorithms. These findings confirm that offloading expensive dominance checks to the edge, governed by an intelligent DRL agent, represents a viable and necessary architectural paradigm for real-time analytics in bandwidth-constrained edge ecosystems.

Future work will focus on three strategic directions to extend the applicability of SA-PSKY. First, we aim to transition from the current single-broker model to a decentralized multi-broker mesh architecture to enhance fault tolerance and scalability in ultra-dense networks. Second, we plan to integrate Federated Learning to enable collaborative policy training across edge nodes while preserving data privacy. This is a critical requirement for sensitive industrial and medical IoT applications. Finally, we will investigate the support for continuous uncertainty models, such as Probability Density Functions, to accommodate more complex physical sensing modalities beyond discrete instance representations.

ACKNOWLEDGMENT

The author would like to thank Wei-Hong Chen for his valuable help with the implementation of the baseline algorithms and data collection.

REFERENCES

- [1] M. Adil, T. Qiu, X. Zhou, D. Javeed, Z. Cao, and D. Oliver Wu, "Integrated 5g and time sensitive networking for emerging applications: A survey of advancements, challenges, and future directions," *IEEE Communications Surveys & Tutorials*, vol. 28, pp. 4016–4050, 2026.
- [2] Q. He, J. Lin, H. Fang, X. Wang, M. Huang, X. Yi, and K. Yu, "Integrating iot and 6g: Applications of edge intelligence, challenges, and future directions," *IEEE Transactions on Services Computing*, vol. 18, no. 4, pp. 2471–2488, 2025.
- [3] N. Yang, S. Chen, H. Zhang, and R. Berry, "Beyond the edge: An advanced exploration of reinforcement learning for mobile edge computing, its applications, and future research trajectories," *IEEE Communications Surveys & Tutorials*, vol. 27, no. 1, pp. 546–594, 2025.
- [4] N. E. H. Boubaker, K. Zarour, N. Guermouche, and D. Benmerzoug, "A comprehensive survey on resource management for iot applications in edge-fog-cloud environments," *IEEE Access*, vol. 13, pp. 111892–111925, 2025.
- [5] J. Pei, B. Jiang, X. Lin, and Y. Yuan, "Probabilistic skylines on uncertain data," in *Proceedings of the 33rd International Conference on Very Large Data Bases*, Vienna, Austria, 2007, pp. 15–26.
- [6] Z. Liu, X. Chen, H. Wu, Z. Wang, X. Chen, D. Niyato, and K. Huang, "Integrated sensing and edge ai: Realizing intelligent perception in 6g," *IEEE Communications Surveys & Tutorials*, vol. 28, pp. 2725–2770, 2026.
- [7] M. Tang, Y. Yu, W. G. Aref, Q. M. Malluhi, and M. Ouzzani, "Efficient parallel skyline query processing for high-dimensional data," *IEEE Transactions on Knowledge and Data Engineering*, vol. 30, no. 10, pp. 1838–1851, 2018.
- [8] F. Song, H. Xing, S. Luo, D. Zhan, P. Dai, and R. Qu, "A multiobjective computation offloading algorithm for mobile-edge computing," *IEEE Internet of Things Journal*, vol. 7, no. 9, pp. 8780–8799, 2020.

[9] Q. Luo, C. Li, T. H. Luan, and W. Shi, "Minimizing the delay and cost of computation offloading for vehicular edge computing," *IEEE Transactions on Services Computing*, vol. 15, no. 5, pp. 2897–2909, 2022.

[10] R. Li, Q. Li, Q. Zou, D. Zhao, X. Zeng, Y. Huang, Y. Jiang, F. Lyu, G. Ormazabal, A. Singh, and H. Schulzrinne, "Iotgemini: Modeling iot network behaviors for synthetic traffic generation," *IEEE Transactions on Mobile Computing*, vol. 23, no. 12, pp. 13 240–13 257, 2024.

[11] D. H. Hussein and M. Ibnkahla, "A novel mathematical framework for modeling application-specific iot traffic," *IEEE Internet of Things Journal*, vol. 11, no. 2, pp. 2364–2381, 2024.

[12] C.-C. Lai, H.-Y. Lin, and C.-M. Liu, "Distributed indexing schemes for k-dominant skyline analytics on uncertain edge-iot data," *IEEE Transactions on Emerging Topics in Computing*, vol. 12, no. 3, pp. 878–890, 2024.

[13] L. Pan, X. Liu, Z. Jia, J. Xu, and X. Li, "A multi-objective clustering evolutionary algorithm for multi-workflow computation offloading in mobile edge computing," *IEEE Transactions on Cloud Computing*, vol. 11, no. 2, pp. 1334–1351, 2023.

[14] X. Zhang, R. Lu, J. Shao, H. Zhu, and A. A. Ghorbani, "Continuous probabilistic skyline query for secure worker selection in mobile crowdsensing," *IEEE Internet of Things Journal*, vol. 8, no. 14, pp. 11 758–11 772, 2021.

[15] C.-C. Lai, T.-C. Wang, C.-M. Liu, and L.-C. Wang, "Probabilistic top- k dominating query monitoring over multiple uncertain iot data streams in edge computing environments," *IEEE Internet of Things Journal*, vol. 6, no. 5, pp. 8563–8576, 2019.

[16] W. Zhang, X. Lin, Y. Zhang, J. Pei, and W. Wang, "Threshold-based probabilistic top-k dominating queries," *The VLDB Journal*, vol. 19, no. 2, pp. 283–305, Apr. 2010.

[17] M. Le, T. Huynh-The, T. Do-Duy, T.-H. Vu, W.-J. Hwang, and Q.-V. Pham, "Applications of distributed machine learning for the internet-of-things: A comprehensive survey," *IEEE Communications Surveys & Tutorials*, vol. 27, no. 2, pp. 1053–1100, 2025.

[18] X. Lian and L. Chen, "Ranked query processing in uncertain databases," *IEEE Transactions on Knowledge and Data Engineering*, vol. 22, no. 3, pp. 420–436, 2010.

[19] M. A. Soliman, I. F. Ilyas, and K. Chen-Chuan Chang, "Top-k query processing in uncertain databases," in *2007 IEEE 23rd International Conference on Data Engineering*, 2007, pp. 896–905.

[20] X. Lin, Y. Yuan, W. Wang, and H. Lu, "Stabbing the sky: efficient skyline computation over sliding windows," in *21st International Conference on Data Engineering (ICDE'05)*, 2005, pp. 502–513.

[21] C.-M. Liu and S.-W. Tang, "An effective probabilistic skyline query process on uncertain data streams," *Procedia Computer Science*, vol. 63, pp. 40–47, 2015.

[22] M. E. Khalefa, M. F. Mokbel, and J. J. Levandoski, "Skyline query processing for incomplete data," in *2008 IEEE 24th International Conference on Data Engineering*, 2008, pp. 556–565.

[23] X. Lian and L. Chen, "Reverse skyline search in uncertain databases," *ACM Transactions on Database Systems*, vol. 35, no. 1, Feb. 2008.

[24] C.-C. Lai, Y.-L. Chen, B.-X. Liu, and C.-M. Liu, "Edge-assisted parallel uncertain skyline processing for low-latency ioe analysis," *IEEE Internet of Things Journal*, vol. 12, no. 21, pp. 44 594–44 611, 2025.

[25] S. Borzsonyi, D. Kossmann, and K. Stocker, "The skyline operator," in *Proceedings 17th International Conference on Data Engineering*, 2001, pp. 421–430.

[26] B. J. Santoso, G.-M. Chiu, and R. Mumpuni, "An efficient grid-based framework for answering tolerance-based skyline queries," in *2015 International Conference on Information & Communication Technology and Systems (ICTS)*, 2015, pp. 251–256.

[27] A. Vlachou, C. Doulkeridis, and Y. Kotidis, "Angle-based space partitioning for efficient parallel skyline computation," in *Proceedings of the 2008 ACM SIGMOD International Conference on Management of Data*, Vancouver, Canada, 2008, pp. 227–238.

[28] B. Cui, L. Chen, L. Xu, H. Lu, G. Song, and Q. Xu, "Efficient skyline computation in structured peer-to-peer systems," *IEEE Transactions on Knowledge and Data Engineering*, vol. 21, no. 7, pp. 1059–1072, 2009.

[29] P. Wu, C. Zhang, Y. Feng, B. Y. Zhao, D. Agrawal, and A. El Abbadi, "Parallelizing skyline queries for scalable distribution," in *Advances in Database Technology - EDBT 2006*, Y. Ioannidis, M. H. Scholl, J. W. Schmidt, F. Matthes, M. Hatzopoulos, K. Boehm, A. Kemper, T. Grust, and C. Boehm, Eds. Berlin, Heidelberg: Springer Berlin Heidelberg, 2006, pp. 112–130.

[30] I.-F. Su, Y.-C. Chung, C. Lee, and Y.-Y. Lin, "Efficient skyline query processing in wireless sensor networks," *Journal of Parallel and Distributed Computing*, vol. 70, no. 6, pp. 680–698, 2010.

[31] A.-T. Kuo, H. Chen, L. Tang, W.-S. Ku, and X. Qin, "Probsky: Efficient computation of probabilistic skyline queries over distributed data," *IEEE Transactions on Knowledge and Data Engineering*, vol. 35, no. 5, pp. 5173–5186, 2023.

[32] H. Wijayanto, W. Wang, W.-S. Ku, and A. L. Chen, "LShape Partitioning: Parallel Skyline Query Processing Using MapReduce," *IEEE Transactions on Knowledge & Data Engineering*, vol. 34, no. 07, pp. 3363–3376, Jul. 2022.

[33] Y. Park, J.-K. Min, and K. Shim, "Efficient processing of skyline queries using mapreduce," *IEEE Transactions on Knowledge and Data Engineering*, vol. 29, no. 5, pp. 1031–1044, 2017.

[34] Z. Xu, G. Xu, H. Wang, W. Liang, Q. Xia, and S. Wang, "Enabling streaming analytics in satellite edge computing via timely evaluation of big data queries," *IEEE Transactions on Parallel and Distributed Systems*, vol. 35, no. 1, pp. 105–122, 2024.

[35] H. Liang, Z. Zhang, C. Hu, Y. Gong, and D. Cheng, "A survey on spatio-temporal big data analytics ecosystem: Resource management, processing platform, and applications," *IEEE Transactions on Big Data*, vol. 10, no. 2, pp. 174–193, 2024.

[36] W. Shi, J. Cao, Q. Zhang, Y. Li, and L. Xu, "Edge computing: Vision and challenges," *IEEE Internet of Things Journal*, vol. 3, no. 5, pp. 637–646, 2016.

[37] M. J. Neely, *Stochastic Network Optimization with Application to Communication and Queueing Systems*, ser. Synthesis Lectures on Communication Networks. Morgan & Claypool Publishers, 2010. [Online]. Available: <https://doi.org/10.2200/S00271ED1V01Y201006CNT007>

[38] T. Nguyen, H. Nguyen, and T. Nguyen Gia, "Exploring the integration of edge computing and blockchain iot: Principles, architectures, security, and applications," *Journal of Network and Computer Applications*, vol. 226, p. 103884, 2024.

[39] X. Kong, Y. Wu, H. Wang, and F. Xia, "Edge computing for internet of everything: A survey," *IEEE Internet of Things Journal*, vol. 9, no. 23, pp. 23 472–23 485, 2022.

[40] M. Ishtiaq, N. Saeed, and M. A. Khan, "Edge computing in the internet of things: A 6g perspective," *IT Professional*, vol. 26, no. 5, pp. 62–70, 2024.

[41] Q. Cai, C. Cui, Y. Xiong, W. Wang, Z. Xie, and M. Zhang, "A survey on deep reinforcement learning for data processing and analytics," *IEEE Transactions on Knowledge and Data Engineering*, vol. 35, no. 5, pp. 4446–4465, 2023.

[42] T. P. Lillicrap, J. J. Hunt, A. Pritzel, N. Heess, T. Erez, Y. Tassa, D. Silver, and D. Wierstra, "Continuous control with deep reinforcement learning," 2019. [Online]. Available: <https://arxiv.org/abs/1509.02971>

[43] X. Gao, X. Xiao, X. Pan, D. Miao, and J. Li, "Efficient algorithms for uncertain restricted skyline query processing," *The VLDB Journal*, vol. 34, no. 4, p. 46, 2025.



Chuan-Chi Lai (Member, IEEE) received the Ph.D. degree in Computer Science and Information Engineering from National Taipei University of Technology, Taipei, Taiwan, in 2017. He was a postdoctoral research fellow (2017–2019) and contract assistant research fellow (2020) with the Department of Electrical and Computer Engineering, National Chiao Tung University, Hsinchu, Taiwan. From Feb. 2021 to Jan. 2024, he served as an assistant professor at the Department of Information Engineering and Computer Science, Feng Chia University, Taichung, Taiwan. From Feb. 2024, he is currently an assistant professor at the Department of Communications Engineering, National Chung Cheng University, Chiayi, Taiwan. He is a member of the IEEE Computer Society, IEEE Communications Society, and IEEE Vehicular Technology Society. His research interests include resource allocation, data management, information dissemination, and distributed query processing for moving objects in emerging applications such as the Internet of Things, edge computing, and next-generation wireless networks. Dr. Lai received the Postdoctoral Researcher Academic Research Award from the Ministry of Science and Technology, Taiwan, in 2019, Best Paper Awards at WOCC 2021 and WOCC 2018, and the Excellent Paper Award at ICUFN 2015.